Design considerations for smartphone camera-based rotational speed measurement

Toby Verwimp, Alexandre Mauricio, Konstantinos Gryllias

Design considerations for smartphone camera-based rotational speed measurement

Toby VERWIMP[1,2], Alexandre MAURICIO[1,2], Konstantinos GRYLLIAS[1,2]

[1]KU Leuven, Department of Mechanical Engineering
LMSD Division Mecha(tro)nic System Dynamics
Celestijnenlaan 300, B-3001, Heverlee, Belgium
[2]Flanders Make@KU Leuven, Belgium
toby.verwimp@kuleuven.be

Abstract

Condition monitoring of rotating machinery gains importance in order to optimally schedule maintenance and to guarantee operation safety and production efficiency. Varying speed conditions are common in rotating machinery operations, but pose a challenge for vibration analysis. Nevertheless, a direct measurement or an indirect estimation of the rotational speed can simplify the monitoring process. Recent studies have shown that a smartphone's low-cost camera can serve as a rotational speed measurement tool, even though it has a low frame rate, by exploiting the rolling shutter effect. In rolling shutter cameras the pixel lines of an image are not sampled simultaneously, but sequentially at a sample rate that is much higher than the frame rate. This rolling shutter frequency results in a very high Nyquist limit allowing for the measurement of high rotational speeds. A recent study proposed a theory and the corresponding methodology to measure the rotational speed of a shaft using a smartphone's rolling shutter camera pointed towards the curved surface of the shaft around which a wide zebra tape was glued. Due to the rolling shutter effect, the stripes are captured as inclined lines of which the angle depends on the rotational speed. The goal of this paper is to investigate and validate the influence of various design parameters, e.g. the dimensions of the zebra tape, on the rotational speed measurement. The design considerations are applied on an in-house experimental drivetrain running at shaft speeds in the range from 5 to 50 revolutions per second and their effect is evaluated in order to conclude with general design rules for smartphone camera-based rotational speed measurement.

1 Introduction

Rotating machinery often operate under varying speed conditions. This complicates vibration analysis, a key element of condition monitoring, as the rotational speed influences the characteristic fault signatures. Therefore, a direct measurement or an indirect estimation of the rotational speed is needed to simplify the monitoring process.

There are several speed measurement sensors available in the market, such as optical encoders, magnetic encoders, and Hall sensors [1]. However, installing these sensors can be expensive and requires a significant amount of space for the sensor, cables and data acquisition system. Recent studies have indicated that high-speed cameras [2, 3, 4] as well as low-cost cameras [5, 6, 7, 8] can be used for rotational speed measurement. However, the measurable speed of low-cost cameras is limited by the Nyquist theorem to half the frame rate, which makes them less effective. Additionally, the temporal resolution of speed measurements is constrained by the inverse of the frame rate, highlighting the superior performance of expensive high-speed cameras. Aside from their high cost, high-speed cameras also require extensive data processing, making them both memory-intensive and time-consuming for speed measurement purposes.

Nowadays, smartphones are ubiquitous due to their versatile use. Cameras in smartphones are also low-cost cameras of which the performance is increasing due to advancements in its electronic and optical components, making them a viable and cost-effective option for speed measurement. However, smartphone video recordings are usually acquired through a rolling shutter instead of a global shutter camera. In order to reduce the cost and to increase the frame rate a rolling shutter camera acquires its pixel rows (or columns) one after the other. This

effect introduces geometrical distortions in the captured scene when there is relative motion between the scene and the smartphone camera. The effect of the distortions on the image quality is more prominent for high-speed motions [9].
Models and calibration techniques have been developed in order to rectify images which are deformed by this rolling shutter effect [10, 11]. However, this effect can also be exploited to extend the measurement capabilities of a rolling shutter camera. As each pixel line is acquired with a specific delay (i.e. the rolling shutter period) and an image consists of thousands of such lines (typically 1080 pixel columns for a smartphone camera), the sampling frequency is three orders higher than the frame rate, allowing for the measurement of fast motions [12, 13].
First efforts have been made to measure rotational speeds of propellers [3] or fans [15] using this rolling shutter effect and have been shown to be very effective since the translational speed of the tip of the blades can get very high resulting in big distortions which can be modelled as a function of the rotational speed. Inspired by the SURVISHNO challenge of 2019 [15], a model and methodology was proposed to measure the speed of a rotating shaft of a drivetrain from the radial side [16] which is usually more accessible than the axial side as in propellers or fans. To apply this model and methodology, some design considerations can be helpful in order to get accurate speed estimations with a smartphone camera.
More specifically, the paper starts with an explanation of the speed estimation model in Section 2.1 for which some design considerations are formulated in Section 2.2. Next, in Section 3.1, the experimental setup is described on which these design considerations are validated in Section 3.2. Finally, Section 4 draws some conclusions and collects key results and findings.

2 Speed estimation through smartphone video acquisition

2.1 Speed estimation model

The model and methodology to estimate the speed from a video of a rotating zebra tape (glued around a shaft) acquired by the rolling shutter camera of a smartphone can be summarized as follows [16] and is shown in Figure 1. The rolling shutter camera captures the pixel columns sequentially from the right to the left with a delay equal to the rolling shutter period τ. During this period the shaft keeps rotating resulting in deformed (inclined) stripes with respect to the original zebra pattern. This deformation with stripe angle α [rad] depends on the Instantanous Angular Speed (IAS) ω [rotations per second, rps], so, reversely, by extracting the deformation from the image of a rotating shaft, its IAS can be estimated by the equation:

$$\omega = \frac{1}{\pi D \tau} \frac{Z}{k_y f_y} (\tan\alpha \cos\beta - \sin\beta) \triangleq A (\tan\alpha \cos\beta - \sin\beta) \tag{1}$$

with D [m] the shaft's diameter, Z [m] the distance between the shaft and the camera, k_y [-] the number of vertical pixels per unit length, f_y the focal length [m], β [rad] a possible misalignment between the rolling shutter direction and the shaft and A [rps] a constant parameter representing a fictitious speed.
With the development of Equation 1, it is assumed that: (i) the zebra pattern is parallel to the image plane, (ii) the speed is constant during the video acquisition of the zebra tape ($\approx$ the acquisition of one image) and (iii) the camera projection is pseudo-orthographic, which is only valid if $\frac{Z}{k_y f_y}$ is constant (i.e. if the captured objects are small compared to their distance from the camera).
Figure 1b shows the overall process to calculate the IAS ω. The video from which the speed needs to be estimated is firstly processed by a user to extract the shaft from its background. From this extraction the misalignment β is estimated. Then in all frames an overall stripe angle α per frame is extracted. Subsequently to estimate the camera parameters, two calibration procedures are followed of which the first one consists of calibrating the camera's intrinsics (Z) and extrinsics ($k_y f_y$) using a video of a checkerboard pattern. The second one consists of measuring the spatial frequency of alternating bright and dark lines in a video of a high-frequency blinking LED light to estimate the rolling shutter period τ.

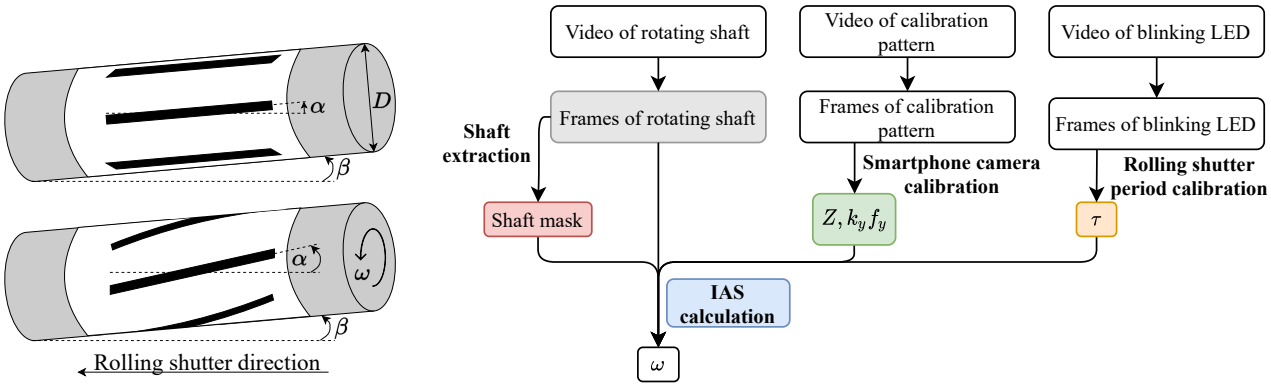

(a) (b)

Figure 1: Speed estimation model: (a) rolling shutter effect on moving zebra pattern and (b) flowchart of the methodology to extract the speed from a radial viewpoint [16]

2.2 Design rules

This section describes three design rules to consider when designing an experiment or setup to measure the rotational speed using the above method, which will be validated in Section 3.2.

2.2.1 Minimum number of stripes

A first design parameter is the number of stripes N_s on the zebra tape. Due to the curvature of the shaft, the assumption that the zebra pattern is parallel to the image plane only holds for the center of the shaft in the image. As it is impossible to extract the stripe angle α from a single line of pixels, a Region Of Interest (ROI) is defined around the shaft's center as shown in Figure 2. This ROI limits the number of stripes that can be captured, especially at low speeds as for high speeds more stripes enter the ROI due to their deformation. Therefore, the worst case scenario is at standstill (i.e. stripes are parallel to ROI). To have at least one stripe in the ROI, the distance d [m] between the stripes is limited by the following equation:

$$d \leq \frac{b}{D_{px}} D \triangleq \tilde{b} D \tag{2}$$

with b the height (in pixels) of the ROI, D_{px} the diameter of the shaft in the image plane and $\tilde{b}$ the height of the ROI normalized with respect to D_{px}. This maximum distance limits the number of stripes N_s to a minimum:

$$N_s \geq \left\lceil \frac{\pi D}{d} \right\rceil = \left\lceil \frac{\pi}{\tilde{b}} \right\rceil \tag{3}$$

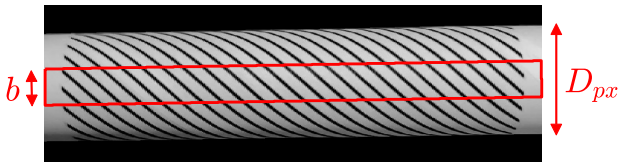

Figure 2: A cropped video frame of a rotating shaft with a zebra pattern and a ROI with height b

2.2.2 Maximum speed

In [16], a first design rule for the maximum IAS was elaborated based on the restriction that the pixels of a stripe need to stay connected to be recognized as one stripe. Figure 3a shows three cases: in the first (green), second (orange) and third (red) case the pixels are respectively well, barely and not connected. Therefore, the IAS is limited to a maximum as during τ a stripe cannot move more than its stripe thickness $t^y_{s,px}$ in the image plane:

$$\omega < \frac{1}{\pi D} \frac{t_s}{\tau \cos^2 \beta} \triangleq \omega_{max,1} \tag{4}$$

with t_s [m] the thickness of a stripe.
Equation 4 results in very high maximum rotational speeds. However, due to the exposure time t_{exp} [s] not being infinitesimally small, the images get blurry (and useless) even before the above limit. To keep the stripes distinguishable (i.e. to limit motion blur), a stripe cannot move to the position of an adjacent stripe during t_{exp}:

$$\begin{aligned} &\Delta\theta_{exp} < \Delta\theta_s \\ \Rightarrow\ &\omega t_{exp} < \frac{1}{N_s} - \frac{t_s}{\pi D} \\ \Rightarrow\ &\omega < \left(\frac{1}{N_s} - \frac{t_s}{\pi D} \right) \frac{1}{t_{exp}} \triangleq \omega_{max,2} \end{aligned} \tag{5}$$

with $\Delta\theta_{exp}$ [rad] the angle travelled during t_{exp} and $\Delta\theta_s$ [rad] the angle between adjacent stripes. From Equation 5 higher speeds can be measured with lower exposure times (as long as a sufficiently strong light source is used). Furthermore the measurable speed limit can be increased by using less stripes (N_s) and decreasing their thickness (t_s).

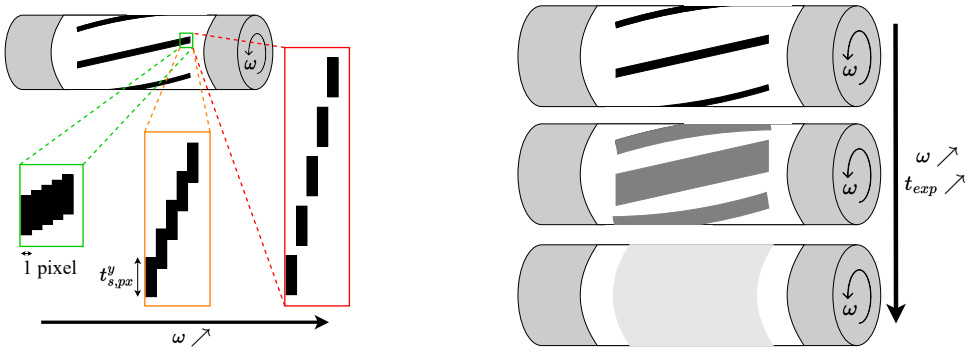

(a) (b)

Figure 3: Approaches to estimate the maximum measurable speed: (a) by keeping the pixels connected to form a stripe and (b) by avoiding too blurry images

2.2.3 Length of zebra tape

A third design rule considers the length of the zebra tape, more specifically its length projected in the image plane. With the current methodology the stripe angle α is estimated from the stripe angle α_i of the two edges (upper and lower) of all stripes in the ROI (Figure 2) by a weighted average:

$$\alpha = \sum_{i=1}^{N_{edges}} w_i \alpha_i = \sum_{i=1}^{N_{edges}} \frac{N_{pixels,i}}{\sum_{i=1}^{N_{edges}} N_{pixels,i}} \alpha_i \tag{6}$$

with the edge weights w_i determined by the amount of pixels $N_{pixels,i}$ of that edge with respect to the total amount of pixels of all edges (N_{edges}) in the ROI. Each stripe angle α_i is determined using linear regression of the edge's pixel coordinates.
As one speed value is estimated for a whole frame period (i.e. inverse of the frame rate), it is important to have contributions from this whole frame period. Therefore, and in order to average out errors in the estimation, the zebra tape should span the entire frame width.

3 Experimental validation of design rules

3.1 Experimental setup

Figure 4 shows the experimental setup which is driven by an open-loop speed-controlled induction motor (1). A flexible coupling (3) connects the motor to the rotating shaft (5) with $D = 0.025$ m which is supported by two healthy bearings (4). The index channel of the incremental rotary encoder (2) is acquired to serve as a reference IAS Ω for the speed estimations ω.
Three different zebra tapes are glued to the shaft. They respectively have 20, 30 and 10 stripes with a thickness of respectively 1 mm, 1 mm and 2 mm and a length of 100 mm. To process the video frames, a ROI with normalized height $\tilde{b} = 1/3$ is used. Therefore the minimum number of stripes is equal to 10.
A flexible smartphone stand (8) allows positioning the smartphone at different distances from the shaft. Next to the smartphone, a tripod is positioned with a microphone (9), which is (together with the encoder) connected to a data acquisition system. The microphone serves as a trigger to start the data acquisition: if the sound pressure exceeds 4 Pa, the acquisition is started. After starting the video recording using a remote button, this pressure can be reached by clapping hands near the microphone. A similar peak is then present in the audio signal of the recorded video, making it possible to synchronize the IAS measurement ω through the video with the reference IAS Ω of the encoder. The camera's frame rate is about 30 fps (frames per second) and its rolling shutter period τ is calibrated to 22.55 µs.
In order to extract the shaft from its background, a red paper (6) is put below the shaft. With the ProCam X smartphone application different exposure times are tested too. For higher speeds, smaller exposure times are needed to avoid blurry images (Equation 5). To capture sufficient light additional light sources (7) are pointed towards the zebra tape.
Next sections describe the experiments and corresponding results for the design rules proposed in Section 2.2.

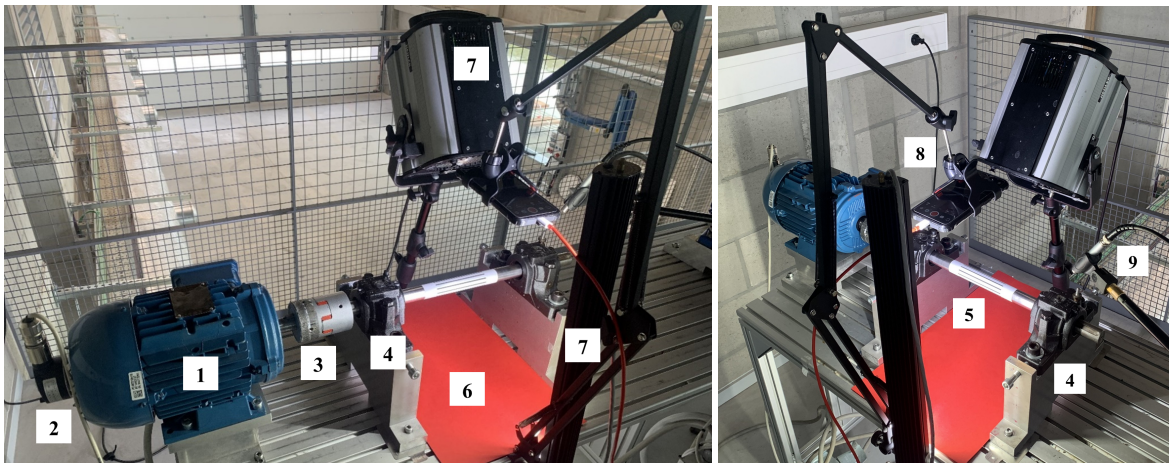

Figure 4: Experimental setup: 1. electric motor, 2. encoder, 3. flexible coupling, 4. bearings, 5. shaft with zebra tape, 6. red background paper, 7. light sources, 8. smartphone held by a flexible support and 9. 1/2" microphone

3.2 Results

3.2.1 Maximum speed

In order to test the design rule to avoid blurry images (Equation 5), the three different zebra tapes are glued to the shaft. The distance between the camera and the shaft is about 0.16 m. For each zebra tape three exposure times t_{exp} are tested of about 500 µs, 1000 µs and 2000 µs respectively. The test parameters, together with the estimations of the maximum speed according to Equations 4 and 5 are shown in Table 1. It follows that image blur will be the limiting factor on the maximum measurable speed.
Figure 5 shows for each test the speed reference Ω and its estimation ω based on the video recordings. The black circle indicates the point at which the estimation ω becomes unreliable. The corresponding speed $\omega_{max,meas}$ at this point is shown in Table 1. N/A (Not Applicable) means that over the full signal the estimation did not suffer

from blurry images. For each zebra tape, doubling the exposure time results in about halving the maximum measurable speed, as expected by Equation 5. Furthermore, for a fixed exposure time, an increase in the number of stripes N_s results in a decrease in the maximum measurable speed. However, the expected maximum speed $\omega_{max,2}$ does not match with the measured one for all tests.
Figure 6 shows four (cropped) video frames of the test corresponding to the second graph of Figure 5a. Video frame 6a is at standstill, video frame 6b at 19 rps (around 10 s), video frame 6c at 31 rps (indicated by the black circle, around 15 s) and video frame 6d is at 50 rps (around 23 s). In Figure 6c the stripes are still (but barely) distinguishable. Therefore, for larger speeds the developed methodology suffers from this bad image quality, which results in inaccurate speed estimations. In Figure 6d the stripes are indistinguishable. The point at which this starts to happen corresponds in Figure 5a to the sudden drop in the speed estimation (i.e. around 18 s and 40 rps) which is already much closer to the estimated maximum speed of 37.8 rps.
Therefore, it can be concluded that before acquiring a completely blurry image, the quality of the images decreases from an earlier point. This quality decrease is detrimental for the speed estimation process. For future designs, this can be circumvented by adding a safety factor (e.g. 2) to Equation 5:

$$2\omega t_{exp} < \frac{1}{N_s} - \frac{t_s}{\pi D} \tag{7}$$

	Tape 1			Tape 2			Tape 3		
N_s [-]	20			30			10		
t_s [mm]	1			1			2		
t_{exp} [µs]	497	987	1979	497	992	1999	499	988	1977
β [°]	0.85	0.90	0.85	0.16	0.19	0.19	0.64	0.58	0.61
$\omega_{max,1}$ [rps]	565	565	565	565	565	565	1129	1129	1129
$\omega_{max,2}$ [rps]	75.0	37.8	18.8	41.4	20.8	10.3	149.3	75.4	37.7
$\omega_{max,meas}$ [rps]	N/A	30	11	45	25	11	N/A	34	19

Table 1: Estimation and measurement of the maximum measurable speed

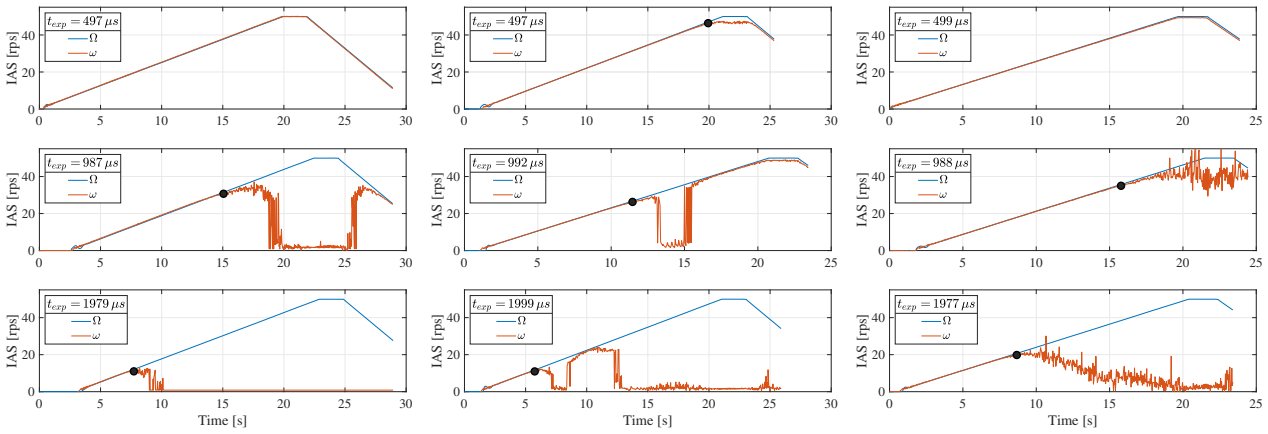

(a) (b) (c)

Figure 5: Speed estimation of a linearly increasing speed profile for different exposure times and zebra tapes: (a) tape 1, (b) tape 2 and (c) tape 3

3.2.2 Length of zebra tape

In order to test the effect of the length of the zebra tape on the quality of the speed estimation, the original ROI (with 1080 pixel columns) shown in Figure 2 is cropped towards the center to ROIs of respectively 800, 400 and 100 pixel columns. The video is recorded with zebra tape 1 glued to the shaft and the smartphone at a distance of about 0.16 m from the shaft. The exposure time is about 100 µs. During the tests a stepwise speed profile is applied with on each step a set of extra small speed increments of about 0.1 rps.

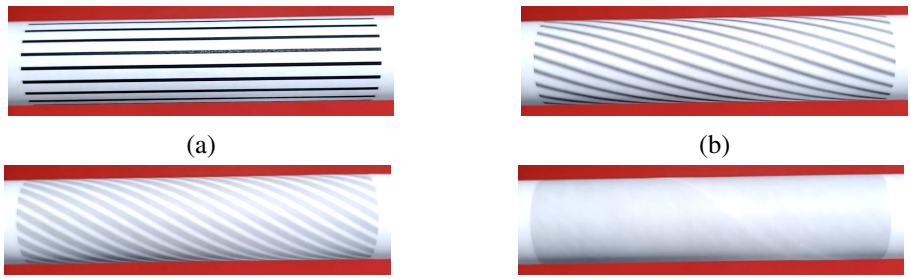

(a) (b) (c) (d)

Figure 6: Video frames of a rotating shaft with zebra tape, corresponding to second graph of Figure 5a: (a) standstill, (b) distinguishable stripes at 19 rps, (c) barely distinguishable stripes at 31 rps and (d) indistinguishable stripes at 50 rps

Figure 7a shows the reference speed together with the four speed estimations corresponding to the number of pixel columns used. The quality of the estimations is still acceptable with Normalized Root-Mean-Square Errors (NRMSE) of respectively 0.49 %, 0.50 %, 0.61 % and 0.72 %. From the zoomed graphs in Figure 7b, the quality difference between the four estimations is visible. Therefore, if possible, the zebra tape should cover the whole image width.

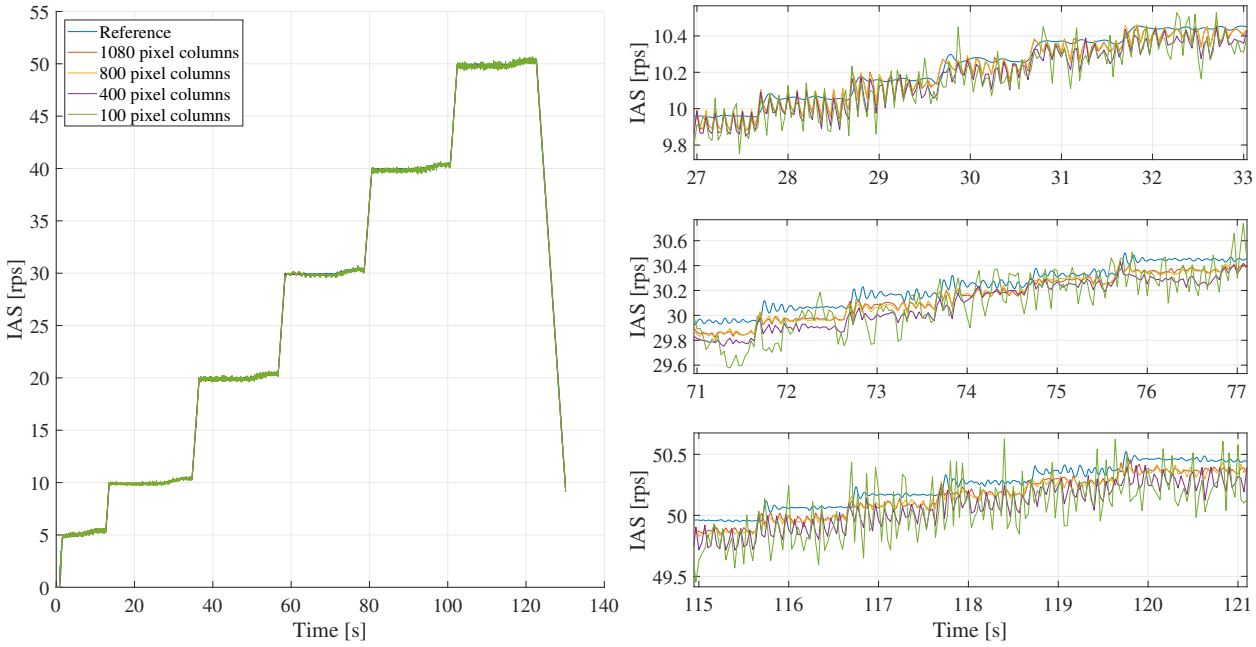

(a) (b)

Figure 7: Speed estimation of a stepwise increasing speed profile with extra small steps in between: (a) full speed profile and (b) zoomed intervals for 10 rps, 30 rps and 50 rps

3.3 Step-by-step design

The design rules proposed in Section 2.2 and tested in Section 3.2 can be combined to a step-by-step procedure (Figure 8) to setup smartphone camera-based rotational speed measurement campaings. Usually, the setup is already constrained in four ways. The shaft diameter D and the available shaft length L depend on the drivetrain itself and can be assumed to be known and fixed. Also the maximum speed depends on the application and can be assumed to be known. Finally, the availability of a light source should also be checked beforehand. The main requirement for the light is to be a DC light source in order to avoid light flickering effects in the images caused by the AC grid frequency.
From Section 3.2.2, the zebra tape should span as many pixel columns as possible, so the smartphone can be positioned at a distance Z. However, it cannot be too close to the shaft due to the assumption that the projection

is pseudo-orthographic. Therefore, as a rule of thumb, the distance Z can be an order higher than D. Next, the exposure time t_{exp} should be chosen in order to have a good contrast of the zebra tape. Thereafter, the number of stripes (and their thickness) can be determined using Equation 7. It should be noted that these design considerations give a first stepping stone to design an experimental setup, but iterations over this process might be needed to converge to a final design. As an example, Figure 9 shows the speed estimation of a stepwise

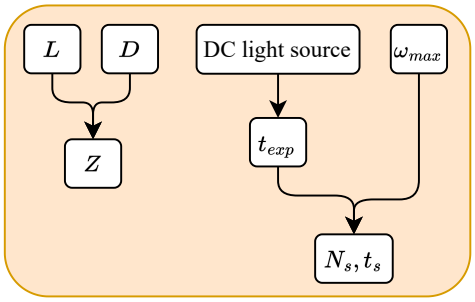

Figure 8: Step-by-step procedure to setup smartphone camera-based rotational speed measurement campaings

increasing speed profile using a smartphone LED as light source. Zebra tape 3 is used and the smartphone is positioned at about 0.2 m (about an order bigger than the diameter). The exposure time is set to about 500 µs. From Equation 7, rotational speeds up to 75 rps should be able to be measured. The NRMSE of the estimation equals 1.46 %, making the measured speed a good estimation for the reference speed. Figure 10 shows a (cropped) video frame for a speed of about 20 rps and the corresponding processed frame with the extracted edges, to get a stripe angle of -7.55°. At first sight, the quality of the image looks bad, but there is still enough contrast in the ROI to distinguish the black stripes from the white paper.

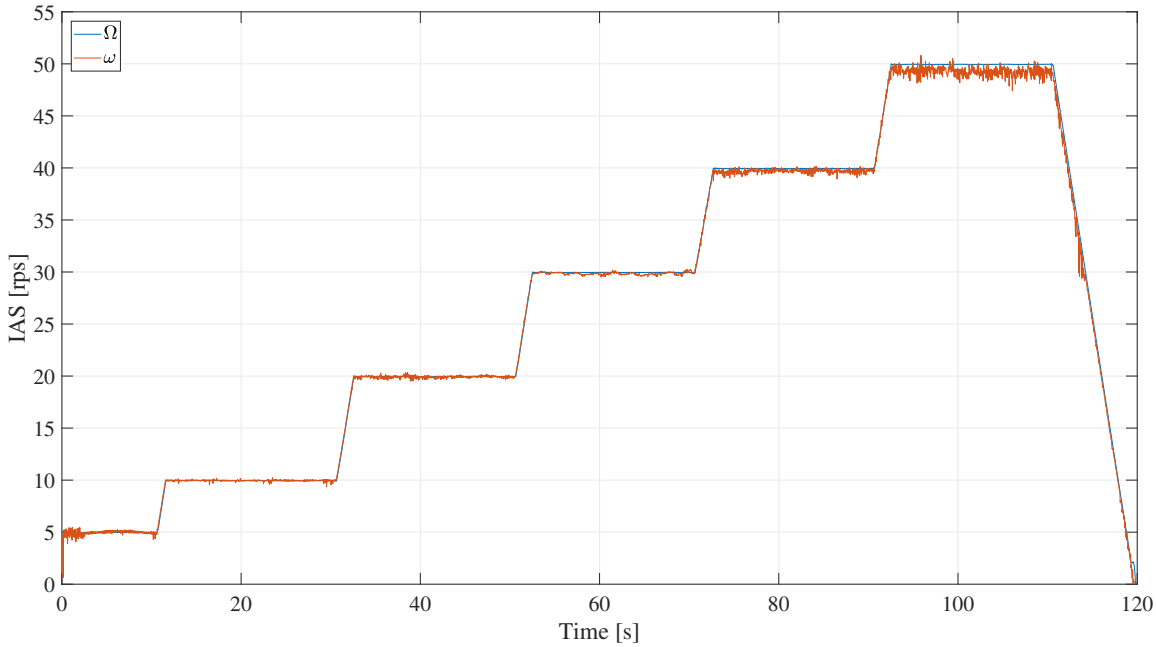

Figure 9: Speed estimation of a stepwise increasing speed profile using a smartphone LED as light source.

(a) (b)

Figure 10: Video frame (cropped) corresponding to Figure 9 for a speed of about 20 rps: (a) original frame with ROI (red) and (b) extracted stripes (white) and edges (green) in the ROI (red)

4 Conclusion

This paper proposed design rules to take into account when setting up a smartphone camera-based rotational speed measurement campaign. The measuring principle is based on measuring the deformation of a zebra tape which is glued to a rotating shaft. The deformation is caused by the rolling shutter effect which is inherent to smartphone cameras and which can be modelled as a function of the rotational speed. In order to measure the speed of a rotating shaft by recording a video the external parameters (position of camera with respect to the shaft) and internal parameters (focus, rolling shutter period) of the camera need to be calibrated. This paper focuses on design considerations for the speed measurement, which are based on the ROI used in the image processing step, the bluriness of the image and the width that the zebra tape spans in the image. Experiments are performed of which the results are used to propose a procedure for the setup of a smartphone camera-based rotational speed measurement campaign.

Acknowledgements

The authors would like to acknowledge the support of the Fonds Wetenschappelijk Onderzoek Vlaanderen (FWO) under the research grant no. 1SE0123N and the Flanders Make, the strategic research center for the manufacturing industry, in the context of the QED project.

References

[1] S. Lu, R. Yan, Y. Liu, Q. Wang, *Tacholess speed estimation in order tracking: A review with application to rotating machine fault diagnosis*, IEEE transactions on instrumentation and measurement, 2019 March 28, Vol. 68, No. 7, pp.2315-2332.

[2] J. Zhong, S. Zhong, Q. Zhang, Z. Peng, S. Liu, Y. Yu, *Vision-based measurement system for instantaneous rotational speed monitoring using linearly varying-density fringe pattern*, IEEE transactions on instrumentation and measurement, 2018 February 8, Vol. 67, No. 6, pp. 1434-1445.

[3] J. Zhong, S. Zhong, Q. Zhang, Z. Peng, *Measurement of instantaneous rotational speed using double-sine-varying-density fringe pattern*, Mechanical systems and signal processing, 2018 March 15, Vol. 103, pp. 117-130.

[4] J. Zhong, S. Zhong, Q. Zhang, N. Maia, Y. Shen, S. Liu, Y. Yu, Z. Peng, *Vision-based system for simultaneous monitoring of shaft rotational speed and axial vibration using non-projection composite fringe pattern*, Mechanical systems and signal processing, 2019 April 1, Vol. 120, pp.765-776.

[5] Y. Wang, L. Wang, Y. Yan, *Rotational speed measurement through digital imaging and image processing*, IEEE International Instrumentation and Measurement Technology Conference (I2MTC), IEEE, Turin, Italy, 2017 May 22-25, pp. 1-6.

[6] T. Wang, L. Wang, Y. Yan, S. Zhang, *Rotational speed measurement using a low-cost imaging device and image processing algorithms*, IEEE International Instrumentation and Measurement Technology Conference (I2MTC), IEEE, Houston, TX, USA, 2018 May 14-17, pp. 1-6.

[7] T. Wang, Y. Yan, L. Wang, Y. Hu, *Rotational speed measurement through image similarity evaluation and spectral analysis*, IEEE access, 2018 August 21, Vol. 6, pp. 46718-46730.

[8] T. Wang, Y. Yan, L. Wang, Y. Hu, S. Zhang, *Instantaneous rotational speed measurement using image correlation and periodicity determination algorithms*, IEEE transactions on instrumentation and measurement, 2019 July 31, Vol. 69, No. 6, pp. 2924-2937.

[9] C.-K. Liang, L.-W. Chang, H. Chen, *Analysis and compensation of rolling shutter effect*, IEEE transactions on image processing, 2008 June 24, Vol. 17, No. 8, pp. 1323-1330.

[10] M. Meingast, C. Geyer, S. Sastry, *Geometric models of rolling-shutter cameras*, Computer Vision and Pattern Recognition, Cornell University, Ithaca, NY, USA, 2005 March 29.

[11] E. Ringaby, E. Ringaby, P.-E. Forssén, *Efficient video rectification and stabilisation for cell-phones*, International journal of computer vision, 2011 June 10, Vol. 96, pp. 335-352.

[12] O. Ait-Aider, N. Andreff, J. M. Lavest, P. Martinet, *Simultaneous object pose and velocity computation using a single view from a rolling shutter camera*, 9th European Conference on Computer Vision, Graz, Austria, 2006 May 7-13, pp. 56-68.

[13] O. Ait-Aider, A. Bartoli, N. Andreff, *Kinematics from lines in a single rolling shutter image*, IEEE Conference on Computer Vision and Pattern Recognition, IEEE, Minneapolis, MN, USA, 2007 June 17-22, pp. 1-6.

[14] Y. Zhao, Y. Li, S. Guo, T. Li, *Measuring the angular velocity of a propeller with video camera using electronic rolling shutter*, Journal of sensors, 2018 March 21, pp. 1-9.

[15] H. André, Q. Leclère, D. Anastasio, Y. Benaïcha, K. Billon, M. Birem, F. Bonnardot, Z. Chin, F. Combet, P. Daems, A. Daga, R. De Geest, B. Elyousfi, J. Griffaton, K. Gryllias, Y. Hawwari, J. Helsen, F. Lacaze, L. Laroche, X. Li, C. Liu, A. Mauricio, A. Melot, A. Ompusunggu, G. Paillot, S. Passos, C. Peeters, M. Perez, J. Qi, E. Sierra-Alonso, W. Smith, X. Thomas, *Using a smartphone camera to analyse rotating and vibrating systems: Feedback on the survishno 2019 contest*, Mechanical systems and signal processing, 2021 June 1, Vol. 154.

[16] T. Verwimp, K. Gryllias., *Rotating Machinery Speed Extraction through Smartphone Video Acquisition*, KU Leuven, Faculty of Engineering Science, Leuven, Belgium, 2021 June.